

Suppression Pattern of Neutral Pions at High Transverse Momentum in Au + Au Collisions at $\sqrt{s_{NN}} = 200$ GeV and Constraints on Medium Transport Coefficients

- A. Adare,⁸ S. Afanasiev,²² C. Aidala,⁹ N. N. Ajitanand,⁴⁹ Y. Akiba,^{43,44} H. Al-Bataineh,³⁸ J. Alexander,⁴⁹ A. Al-Jamel,³⁸ K. Aoki,^{28,43} L. Aphecetche,⁵¹ R. Armendariz,³⁸ S. H. Aronson,³ J. Asai,⁴⁴ E. T. Atomssa,²⁹ R. Averbeck,⁵⁰ T. C. Awes,³⁹ B. Azmoun,³ V. Babintsev,¹⁸ G. Baksay,¹⁴ L. Baksay,¹⁴ A. Baldissari,¹¹ K. N. Barish,⁴ P. D. Barnes,³¹ B. Bassalleck,³⁷ S. Bathe,⁴ S. Batsouli,^{9,39} V. Baublis,⁴² F. Bauer,⁴ A. Bazilevsky,³ S. Belikov,^{3,21,*} R. Bennett,⁵⁰ Y. Berdnikov,⁴⁶ A. A. Bickley,⁸ M. T. Bjorndal,⁹ J. G. Boissevain,³¹ H. Borel,¹¹ K. Boyle,⁵⁰ M. L. Brooks,³¹ D. S. Brown,³⁸ D. Bucher,³⁴ H. Buesching,³ V. Bumazhnov,¹⁸ G. Bunce,^{3,44} J. M. Burward-Hoy,³¹ S. Butsyk,^{31,50} S. Campbell,⁵⁰ J.-S. Chai,²³ B. S. Chang,⁵⁸ J.-L. Charvet,¹¹ S. Chernichenko,¹⁸ J. Chiba,²⁴ C. Y. Chi,⁹ M. Chiu,^{9,19} I. J. Choi,⁵⁸ T. Chujo,⁵⁵ P. Chung,⁴⁹ A. Churyn,¹⁸ V. Cianciolo,³⁹ C. R. Cleven,¹⁶ Y. Cobigo,¹¹ B. A. Cole,⁹ M. P. Comets,⁴⁰ P. Constantin,^{21,31} M. Csanad,¹³ T. Cs org o,²⁵ T. Dahms,⁵⁰ K. Das,¹⁵ G. David,³ M. B. Deaton,¹ K. Dehmelt,¹⁴ H. Delagrange,⁵¹ A. Denisov,¹⁸ D. d'Enterria,⁹ A. Deshpande,^{44,50} E. J. Desmond,³ O. Dietzsch,⁴⁷ A. Dion,⁵⁰ M. Donadelli,⁴⁷ J. L. Drachenberg,¹ O. Drapier,²⁹ A. Drees,⁵⁰ A. K. Dubey,⁵⁷ A. Durum,¹⁸ V. Dzhordzhadze,^{4,52} Y. V. Efremenko,³⁹ J. Egdemir,⁵⁰ F. Ellinghaus,⁸ W. S. Emam,⁴ A. Enokizono,^{17,30} H. En'yo,^{43,44} B. Espagnon,⁴⁰ S. Esumi,⁵⁴ K. O. Eyser,⁴ D. E. Fields,^{37,44} M. Finger,^{5,22} M. Finger, Jr.,^{5,22} F. Fleuret,²⁹ S. L. Fokin,²⁷ B. Forestier,³² Z. Fraenkel,^{57,*} J. E. Frantz,^{9,50} A. Franz,³ A. D. Frawley,¹⁵ K. Fujiwara,⁴³ Y. Fukao,^{28,43} S.-Y. Fung,⁴ T. Fusayasu,³⁶ S. Gadrat,³² I. Garishvili,⁵² F. Gastineau,⁵¹ M. Germain,⁵¹ A. Glenn,^{8,52} H. Gong,⁵⁰ M. Gonin,²⁹ J. Gosset,¹¹ Y. Goto,^{43,44} R. Granier de Cassagnac,²⁹ N. Grau,²¹ S. V. Greene,⁵⁵ M. Grosse Perdekamp,^{19,44} T. Gunji,⁷ H.-A. Gustafsson,³³ T. Hachiya,^{17,43} A. Hadj Henni,⁵¹ C. Haegemann,³⁷ J. S. Haggerty,³ M. N. Hagiwara,¹ H. Hamagaki,⁷ R. Han,⁴¹ H. Harada,¹⁷ E. P. Hartouni,³⁰ K. Haruna,¹⁷ M. Harvey,³ E. Haslum,³³ K. Hasuko,⁴³ R. Hayano,⁷ M. Heffner,³⁰ T. K. Hemmick,⁵⁰ T. Hester,⁴ J. M. Heuser,⁴³ X. He,¹⁶ H. Hiejima,¹⁹ J. C. Hill,²¹ R. Hobbs,³⁷ M. Hohlmann,¹⁴ M. Holmes,⁵⁵ W. Holzmann,⁴⁹ K. Homma,¹⁷ B. Hong,²⁶ T. Horaguchi,^{43,53} D. Hornback,⁵² M. G. Hur,²³ T. Ichihara,^{43,44} K. Imai,^{28,43} J. Imrek,¹² M. Inaba,⁵⁴ Y. Inoue,^{45,43} D. Isenhower,¹ L. Isenhower,¹ M. Ishihara,⁴³ T. Isobe,⁷ M. Issah,⁴⁹ A. Isupov,²² B. V. Jacak,^{50,+} J. Jia,⁹ J. Jin,⁹ O. Jinnouchi,⁴⁴ B. M. Johnson,³ K. S. Joo,³⁵ D. Jouan,⁴⁰ F. Kajihara,^{7,43} S. Kametani,^{7,56} N. Kamihara,^{43,53} J. Kamin,⁵⁰ M. Kaneta,⁴⁴ J. H. Kang,⁵⁸ H. Kanou,^{43,53} T. Kawagishi,⁵⁴ D. Kawall,⁴⁴ A. V. Kazantsev,²⁷ S. Kelly,⁸ A. Khanzadeev,⁴² J. Kikuchi,⁵⁶ D. H. Kim,³⁵ D. J. Kim,⁵⁸ E. Kim,⁴⁸ Y.-S. Kim,²³ E. Kinney,⁸ A. Kiss,¹³ E. Kistenev,³ A. Kiyomichi,⁴³ J. Klay,³⁰ C. Klein-Boesing,³⁴ L. Kochenda,⁴² V. Kochetkov,¹⁸ B. Komkov,⁴² M. Konno,⁵⁴ D. Kotchetkov,⁴ A. Kozlov,⁵⁷ A. Kr  l,¹⁰ A. Kravitz,⁹ P. J. Kroon,³ J. Kubart,^{5,20} G. J. Kunde,³¹ N. Kurihara,⁷ K. Kurita,^{45,43} M. J. Kweon,²⁶ Y. Kwon,^{52,58} G. S. Kyle,³⁸ R. Lacey,⁴⁹ Y.-S. Lai,⁹ J. G. Lajoie,²¹ A. Lebedev,²¹ Y. Le Bornec,⁴⁰ S. Leckey,⁵⁰ D. M. Lee,³¹ M. K. Lee,⁵⁸ T. Lee,⁴⁸ M. J. Leitch,³¹ M. A. L. Leite,⁴⁷ B. Lenzi,⁴⁷ H. Lim,⁴⁸ T. Li  ka,¹⁰ A. Litvinenko,²² M. X. Liu,³¹ X. Li,⁶ X. H. Li,⁴ B. Love,⁵⁵ D. Lynch,³ C. F. Maguire,⁵⁵ Y. I. Makdisi,³ A. Malakhov,²² M. D. Malik,³⁷ V. I. Manko,²⁷ Y. Mao,^{41,43} L. Ma  ek,^{5,20} H. Masui,⁵⁴ F. Matathias,^{9,50} M. C. McCain,¹⁹ M. McCumber,⁵⁰ P. L. McGaughey,³¹ Y. Miake,⁵⁴ P. Mike  s,^{5,20} K. Miki,⁵⁴ T. E. Miller,⁵⁵ A. Milov,⁵⁰ S. Mioduszewski,³ G. C. Mishra,¹⁶ M. Mishra,² J. T. Mitchell,³ M. Mitrofski,⁴⁹ A. Morreale,⁴ D. P. Morrison,³ J. M. Moss,³¹ T. V. Moukhanova,²⁷ D. Mukhopadhyay,⁵⁵ J. Murata,^{45,43} S. Nagamiya,²⁴ Y. Nagata,⁵⁴ J. L. Nagle,⁸ M. Naglis,⁵⁷ I. Nakagawa,^{43,44} Y. Nakamiya,¹⁷ T. Nakamura,¹⁷ K. Nakano,^{43,53} J. Newby,³⁰ M. Nguyen,⁵⁰ B. E. Norman,³¹ A. S. Nyanin,²⁷ J. Nystrand,³³ E. O'Brien,³ S. X. Oda,⁷ C. A. Ogilvie,²¹ H. Ohnishi,⁴³ I. D. Ojha,⁵⁵ H. Okada,^{28,43} K. Okada,⁴⁴ M. Oka,⁵⁴ O. O. Omiwade,¹ A. Oskarsson,³³ I. Otterlund,³³ M. Ouchida,¹⁷ K. Ozawa,⁷ R. Pak,³ D. Pal,⁵⁵ A. P. T. Palounek,³¹ V. Pantuev,⁵⁰ V. Papavassiliou,³⁸ J. Park,⁴⁸ W. J. Park,²⁶ S. F. Pate,³⁸ H. Pei,²¹ J.-C. Peng,¹⁹ H. Pereira,¹¹ V. Peresedov,²² D. Yu. Peressounko,²⁷ C. Pinkenburg,³ R. P. Pisani,³ M. L. Purschke,³ A. K. Purwar,^{31,50} H. Qu,¹⁶ J. Rak,^{21,37} A. Rakotozafindrabe,²⁹ I. Ravinovich,⁵⁷ K. F. Read,^{39,52} S. Rembeczki,¹⁴ M. Reuter,⁵⁰ K. Reygers,³⁴ V. Riabov,⁴² Y. Riabov,⁴² G. Roche,³² A. Romana,^{29,*} M. Rosati,²¹ S. S. E. Rosendahl,³³ P. Rosnet,³² P. Rukoyatkin,²² V. L. Rykov,⁴³ S. S. Ryu,⁵⁸ B. Sahlmueller,³⁴ N. Saito,^{28,43,44} T. Sakaguchi,^{3,7,56} S. Sakai,⁵⁴ H. Sakata,¹⁷ V. Samsonov,⁴² H. D. Sato,^{28,43} S. Sato,^{3,24,54} S. Sawada,²⁴ J. Seele,⁸ R. Seidl,¹⁹ V. Semenov,¹⁸ R. Seto,⁴ D. Sharma,⁵⁷ T. K. Shea,³ I. Shein,¹⁸ A. Shevel,^{42,49} T.-A. Shibata,^{43,53} K. Shigaki,¹⁷ M. Shimomura,⁵⁴ T. Shohjoh,⁵⁴ K. Shoji,^{28,43} A. Sickles,⁵⁰ C. L. Silva,⁴⁷ D. Silvermyr,³⁹ C. Silvestre,¹¹ K. S. Sim,²⁶ C. P. Singh,² V. Singh,² S. Skutnik,²¹ M. Slune  ka,^{5,22} W. C. Smith,¹ A. Soldatov,¹⁸ R. A. Soltz,³⁰ W. E. Sondheim,³¹ S. P. Sorensen,⁵² I. V. Sourikova,³ F. Staley,¹¹ P. W. Stankus,³⁹ E. Stenlund,³³ M. Stepanov,³⁸ A. Ster,²⁵ S. P. Stoll,³ T. Sugitate,¹⁷ C. Suire,⁴⁰ J. P. Sullivan,³¹ J. Sziklai,²⁵ T. Tabaru,⁴⁴ S. Takagi,⁵⁴ E. M. Takagui,⁴⁷ A. Takeuchi,^{43,44} K. H. Tanaka,²⁴ Y. Tanaka,³⁶ K. Tanida,^{43,44} M. J. Tannenbaum,³ A. Tarantenko,⁴⁹ P. Tarj  n,¹² T. L. Thomas,³⁷

M. Togawa,^{28,43} A. Toia,⁵⁰ J. Tojo,⁴³ L. Tomášek,²⁰ H. Torii,⁴³ R. S. Towell,¹ V-N. Tram,²⁹ I. Tserruya,⁵⁷
Y. Tsuchimoto,^{17,43} S. K. Tuli,² H. Tydesjö,³³ N. Tyurin,¹⁸ C. Vale,²¹ H. Valle,⁵⁵ H. W. van Hecke,³¹ J. Velkovska,⁵⁵
R. Vertesi,¹² A. A. Vinogradov,²⁷ M. Virius,¹⁰ V. Vrba,²⁰ E. Vznuzdaev,⁴² M. Wagner,^{28,43} D. Walker,⁵⁰ X. R. Wang,³⁸
Y. Watanabe,^{43,44} J. Wessels,³⁴ S. N. White,³ N. Willis,⁴⁰ D. Winter,⁹ C. L. Woody,³ M. Wysocki,⁸ W. Xie,^{4,44}
Y. L. Yamaguchi,⁵⁶ A. Yanovich,¹⁸ Z. Yasin,⁴ J. Ying,¹⁶ S. Yokkaichi,^{43,44} G. R. Young,³⁹ I. Younus,³⁷ I. E. Yushmanov,²⁷
W. A. Zajc,⁹ O. Zaudtke,³⁴ C. Zhang,^{9,39} S. Zhou,⁶ J. Zimányi,^{25,*} and L. Zolin²²

(PHENIX Collaboration)

¹Abilene Christian University, Abilene, Texas 79699, USA

²Department of Physics, Banaras Hindu University, Varanasi 221005, India

³Brookhaven National Laboratory, Upton, New York 11973-5000, USA

⁴University of California-Riverside, Riverside, California 92521, USA

⁵Charles University, Ovocný trh 5, Praha 1, 116 36, Prague, Czech Republic

⁶China Institute of Atomic Energy (CIAE), Beijing, People's Republic of China

⁷Center for Nuclear Study, Graduate School of Science, University of Tokyo, 7-3-1 Hongo, Bunkyo, Tokyo 113-0033, Japan

⁸University of Colorado, Boulder, Colorado 80309, USA

⁹Columbia University, New York, New York 10027 and Nevis Laboratories, Irvington, New York 10533, USA

¹⁰Czech Technical University, Zikova 4, 166 36 Prague 6, Czech Republic

¹¹Dapnia, CEA Saclay, F-91191, Gif-sur-Yvette, France

¹²Debrecen University, H-4010 Debrecen, Egyetem tér 1, Hungary

¹³ELTE, Eötvös Loránd University, H-1117 Budapest, Pázmány P. s. 1/A, Hungary

¹⁴Florida Institute of Technology, Melbourne, Florida 32901, USA

¹⁵Florida State University, Tallahassee, Florida 32306, USA

¹⁶Georgia State University, Atlanta, Georgia 30303, USA

¹⁷Hiroshima University, Kagamiyama, Higashi-Hiroshima 739-8526, Japan

¹⁸IHEP Protvino, State Research Center of Russian Federation, Institute for High Energy Physics, Protvino, 142281, Russia

¹⁹University of Illinois at Urbana-Champaign, Urbana, Illinois 61801, USA

²⁰Institute of Physics, Academy of Sciences of the Czech Republic, Na Slovance 2, 182 21 Prague 8, Czech Republic

²¹Iowa State University, Ames, Iowa 50011, USA

²²Joint Institute for Nuclear Research, 141980 Dubna, Moscow Region, Russia

²³KAERI, Cyclotron Application Laboratory, Seoul, Korea

²⁴KEK, High Energy Accelerator Research Organization, Tsukuba, Ibaraki 305-0801, Japan

²⁵KFKI Research Institute for Particle and Nuclear Physics of the Hungarian Academy of Sciences (MTA KFKI RMKI),

H-1525 Budapest 114, POBox 49, Budapest, Hungary

²⁶Korea University, Seoul, 136-701, Korea

²⁷Russian Research Center "Kurchatov Institute", Moscow, Russia

²⁸Kyoto University, Kyoto 606-8502, Japan

²⁹Laboratoire Leprince-Ringuet, Ecole Polytechnique, CNRS-IN2P3, Route de Saclay, F-91128, Palaiseau, France

³⁰Lawrence Livermore National Laboratory, Livermore, California 94550, USA

³¹Los Alamos National Laboratory, Los Alamos, New Mexico 87545, USA

³²LPC, Université Blaise Pascal, CNRS-IN2P3, Clermont-Fd, 63177 Aubiere Cedex, France

³³Department of Physics, Lund University, Box 118, SE-221 00 Lund, Sweden

³⁴Institut für Kernphysik, University of Muenster, D-48149 Muenster, Germany

³⁵Myongji University, Yongin, Kyonggido 449-728, Korea

³⁶Nagasaki Institute of Applied Science, Nagasaki-shi, Nagasaki 851-0193, Japan

³⁷University of New Mexico, Albuquerque, New Mexico 87131, USA

³⁸New Mexico State University, Las Cruces, New Mexico 88003, USA

³⁹Oak Ridge National Laboratory, Oak Ridge, Tennessee 37831, USA

⁴⁰IPN-Orsay, Université Paris Sud, CNRS-IN2P3, BP1, F-91406, Orsay, France

⁴¹Peking University, Beijing, People's Republic of China

⁴²PNPI, Petersburg Nuclear Physics Institute, Gatchina, Leningrad region, 188300, Russia

⁴³RIKEN, The Institute of Physical and Chemical Research, Wako, Saitama 351-0198, Japan

⁴⁴RIKEN BNL Research Center, Brookhaven National Laboratory, Upton, New York 11973-5000, USA

⁴⁵Physics Department, Rikkyo University, 3-34-1 Nishi-Ikebukuro, Toshima, Tokyo 171-8501, Japan

⁴⁶Saint Petersburg State Polytechnic University, St. Petersburg, Russia

⁴⁷Universidade de São Paulo, Instituto de Física, Caixa Postal 66318, São Paulo CEP05315-970, Brazil

⁴⁸System Electronics Laboratory, Seoul National University, Seoul, Korea

⁴⁹Chemistry Department, Stony Brook University, SUNY, Stony Brook, New York 11794-3400, USA

⁵⁰*Department of Physics and Astronomy, Stony Brook University, SUNY, Stony Brook, New York 11794, USA*⁵¹*SUBATECH (Ecole des Mines de Nantes, CNRS-IN2P3, Université de Nantes) BP 20722-44307, Nantes, France*⁵²*University of Tennessee, Knoxville, Tennessee 37996, USA*⁵³*Department of Physics, Tokyo Institute of Technology, Oh-okayama, Meguro, Tokyo 152-8551, Japan*⁵⁴*Institute of Physics, University of Tsukuba, Tsukuba, Ibaraki 305, Japan*⁵⁵*Vanderbilt University, Nashville, Tennessee 37235, USA*⁵⁶*Waseda University, Advanced Research Institute for Science and Engineering, 17 Kikui-cho, Shinjuku-ku, Tokyo 162-0044, Japan*⁵⁷*Weizmann Institute, Rehovot 76100, Israel*⁵⁸*Yonsei University, IPAP, Seoul 120-749, Korea*

(Received 25 January 2008; published 3 December 2008)

For Au + Au collisions at 200 GeV, we measure neutral pion production with good statistics for transverse momentum, p_T , up to 20 GeV/c. A fivefold suppression is found, which is essentially constant for $5 < p_T < 20$ GeV/c. Experimental uncertainties are small enough to constrain any model-dependent parametrization for the transport coefficient of the medium, e.g., $\langle \hat{q} \rangle$ in the parton quenching model. The spectral shape is similar for all collision classes, and the suppression does not saturate in Au + Au collisions.

DOI: 10.1103/PhysRevLett.101.232301

PACS numbers: 25.75.Dw

Large transverse momentum (p_T) hadrons originate primarily from the fragmentation of hard scattered quarks or gluons. In high energy $p + p$ collisions, this is well described in the framework of perturbative QCD [1]. In ultrarelativistic heavy ion collisions, such hard scatterings occur in the early phase of the reaction, and the transiting partons serve as probes of the strongly interacting medium produced in the collisions. Lattice QCD predicts a phase transition to a plasma of deconfined quarks and gluons, which induces gluon radiation from the scattered parton and depletes hadron production at high p_T (“jet quenching”) [2,3]. The measurements in Au + Au collisions at Relativistic Heavy Ion Collider (RHIC) showed suppressed hadron yields in central collisions [4] as predicted [5,6], and motivated advanced theoretical studies of radiative energy loss.

All energy loss models must incorporate the space-time evolution of the medium, as it is not static, and the initial distribution of the partons throughout the medium. Models generally also include an input parameter for the medium density and/or the coupling. Different assumptions in the various models lead to similar descriptions of the π^0 suppression with different model-dependent parameters [7,8]. For instance, the Parton Quenching model (PQM) is a Monte Carlo program using the quenching weights from Baier-Dokshitzer-Mueller-Peigne-Schiff (BDMPS) [5] that combines the coupling strength with the color-charge density to create a single transport coefficient, often referred to as $\langle \hat{q} \rangle$ [9,10], which gives the $\langle p_T^2 \rangle$ transferred from the medium to the parton per mean free path.

Establishing the magnitude, p_T and centrality dependence of the suppression pattern up to the highest possible p_T is crucial to constrain the theoretical models and separate contributions of initial and final state effects from the energy loss mechanism. As neutral pions can be identified up to very high p_T , their suppression and its centrality (average pathlength) dependence puts important con-

straints on the energy loss. Whereas di-hadron suppression at high p_T may be somewhat more sensitive to medium opacity [11] than single hadron suppression, such improvement is contingent upon theoretical and experimental, statistical and systematic uncertainties.

This Letter reports on the measurement of π^0 s up to $p_T = 20$ GeV/c in Au + Au collisions at $\sqrt{s_{NN}} = 200$ GeV at RHIC, using the high statistics data taken in 2004. The results are used to extract the $\langle \hat{q} \rangle$ parameter of the PQM model for the most central collisions.

The analysis used 1.03×10^9 minimum bias events taken by the PHENIX experiment [12]. Collision centrality was determined from the correlation between the number of charged particles detected in the Beam-Beam Counters (BBC, $3.0 < |\eta| < 3.9$) and the energy measured in the Zero Degree Calorimeters (ZDC). A Glauber model Monte Carlo program with a simulation of the BBC and ZDC responses was used to estimate the average number of participating nucleons ($\langle N_{\text{part}} \rangle$) and binary nucleon-nucleon collisions ($\langle N_{\text{coll}} \rangle$) for each centrality bin [13].

Neutral pions were measured in the $\pi^0 \rightarrow \gamma\gamma$ decay channel with the photons reconstructed in the Electromagnetic Calorimeter (EMCal) located in the two central arms of PHENIX ($|\eta| \leq 0.35$). The EMCal [14] consists of two subsystems: six sectors of lead-scintillator sandwich calorimeter (PbSc) and two sectors of lead-glass Čerenkov calorimeter (PbGl) at the radial distance of about 5 m. The fine segmentation of the EMCal ($\delta\phi \times \delta\eta \sim 0.01 \times 0.01$ for PbSc and $\sim 0.008 \times 0.008$ for PbGl) ensures that the two photons from a $\pi^0 \rightarrow \gamma\gamma$ decay are well resolved up to $p_T^{\pi^0} \approx 12$ (PbSc) and 16 (PbGl) GeV/c. Data from the two subsystems were analyzed separately, and the fully corrected results were combined.

Details of the analysis including extraction of the raw π^0 yield, correction for acceptance, detector response, reconstruction efficiency have been described elsewhere [15,16]. In this analysis, the higher p_T range required an additional

TABLE I. Summary of the systematic uncertainties on the π^0 yield extracted independently with the PbSc (PbGl) electromagnetic calorimeters. The last row is the total systematic uncertainty on the combined spectra.

p_T (GeV/c)	2	6	10	16
uncertainty source	PbSc (PbGl)			
yield extraction (%)	3.0 (4.1)	3.0 (4.1)	3.0 (4.1)	3.0 (4.1)
PID efficiency (%)	3.5 (3.9)	3.5 (3.5)	3.5 (3.7)	3.5 (3.9)
Energy scale (%)	6.7 (9.0)	8.0 (9.2)	8.0 (8.2)	8.0 (12.3)
Acceptance (%)	1.5 (4.1)	1.5 (4.1)	1.5 (4.1)	1.5 (4.1)
π^0 merging (%)	... (....)	... (....)	4.4 (....)	28 (4.8)
Conversion (%)	3.0 (2.5)	3.0 (2.5)	3.0 (2.5)	3.0 (2.5)
off-vertex π^0 (%)	1.5 (1.5)	1.5 (1.5)	1.5 (1.5)	1.5 (1.5)
Total (%)	8.7 (12)	9.8 (11)	11 (11)	30 (15)
PbSc and PbGl combined: Total (%)	7.0	7.5	7.6	14

correction for losses in the observed (raw) π^0 s due to “cluster merging.”

With increasing $p_T^{\pi^0}$, the minimum opening angle of the two photons decreases, and eventually they will be reconstructed as a single cluster. Such “merging” reaches 50% of the total raw yield at $p_T = 14$ GeV/c in the PbSc and at $p_T = 18$ GeV/c in the PbGl. Merged clusters were rejected by various shower profile cuts, and the loss was determined by simulated π^0 s embedded into real events and analyzed with the same cuts. The systematic uncertainties were estimated by comparing π^0 yields in the PbSc extracted in bins of asymmetry $|E_{\gamma_1} - E_{\gamma_2}|/(E_{\gamma_1} + E_{\gamma_2})$ and also by comparing yields in the PbSc and PbGl.

We considered two sources of π^0 s not coming from the vertex (off-vertex π^0): those produced by hadrons interacting with detector material (instrumental background) and feed-down products from weak decay of higher mass hadrons (physics background). Based upon simulations both types of background were found to be negligible ($< 1\%$ at $p_T > 2.0$ GeV/c) except for π^0 s from K_S^0 decay ($\approx 3\%$ of π^0 yield for $p_T > 1$ GeV/c), which has been subtracted from the data. Finally, the yields were corrected to the center of the p_T bins using the local slope.

The main sources of systematic uncertainties are yield extraction, efficiency corrections, energy scale, and merging, none of which exhibits a significant centrality dependence. The PbSc and PbGl have quite different systematics with all but one of them (off-vertex π^0) uncorrelated. Therefore, when combining their results, the total error is reduced in the weighted average of the two independent measurements. The final systematic uncertainties (1 standard deviation) on the spectra are shown in Table I.

The top panel of Fig. 1 shows the π^0 invariant yield for all centralities and minimum bias, combined from the independent PbSc and PbGl measurements which now extend to $p_T \sim 20$ GeV/c, 6 GeV/c higher than those published earlier [15]. In the overlap region, the results are consistent with the ones in [15] while the errors are reduced by a factor of 2 to 2.5. The bottom panel shows the

consistency of the PbSc and PbGl results. The spectra are similar at all centralities: when fitting $p_T > 5$ GeV/c with a power-law function ($\propto p_T^{-n}$), the exponents vary from $n = 8.00 \pm 0.12$ in 0–5% to $n = 8.06 \pm 0.08$ in the 80–92% (most peripheral) bin. Note that $n = 8.22 \pm 0.09$ in $p + p$ collisions. The errors are combined statistical errors and systematic uncertainties.

To quantify the comparison of spectra in heavy ion and $p + p$ collisions, the nuclear modification factor

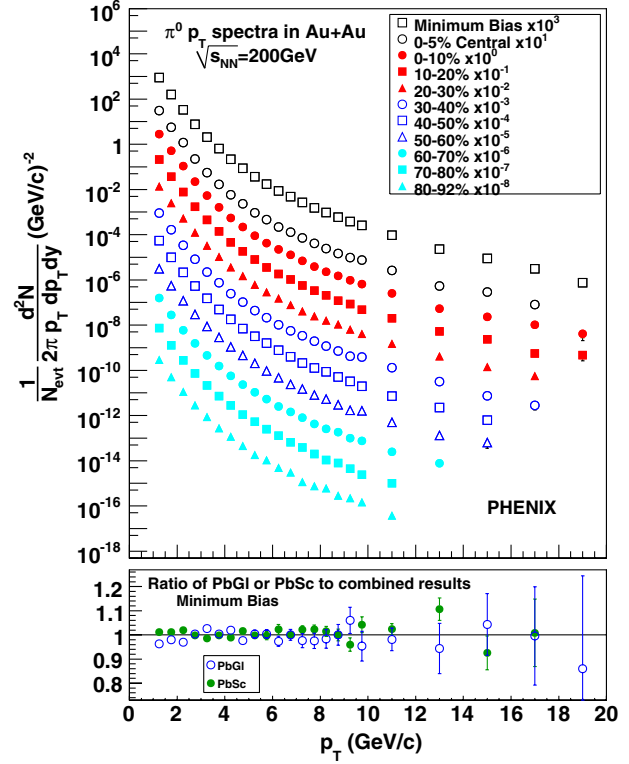


FIG. 1 (color online). Top: π^0 invariant yields for all centralities and minimum bias. Bottom: ratios of the (separately analyzed) PbSc and PbGl yields to the combined minimum bias invariant yield, which is shown in the top panel.

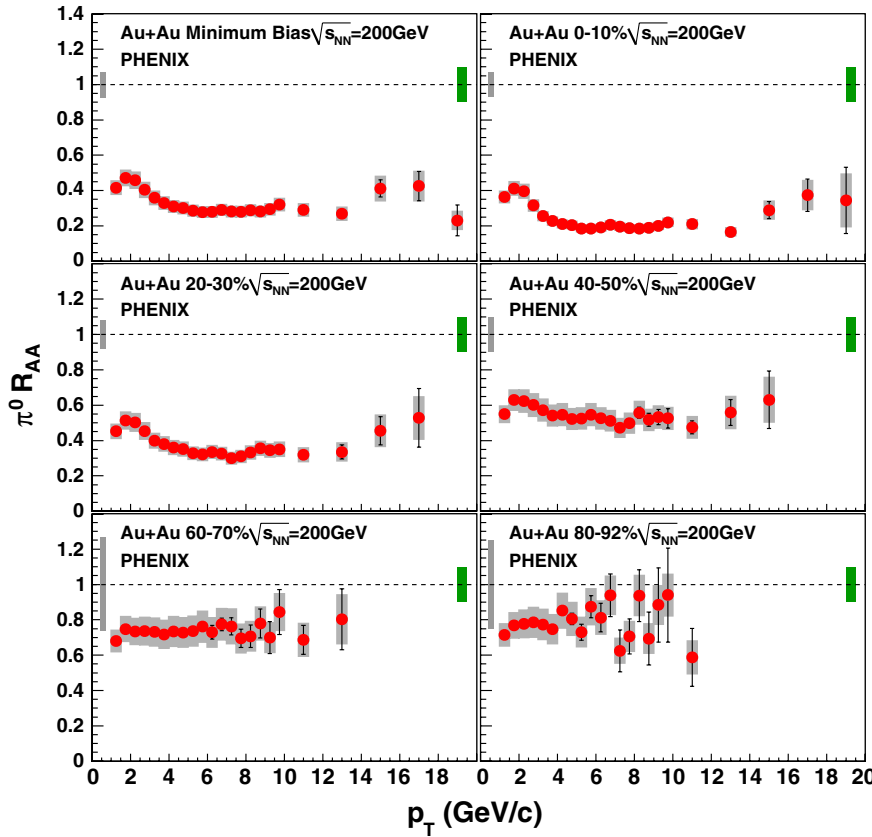


FIG. 2 (color online). Nuclear modification factor (R_{AA}) for π^0 s. Error bars are statistical and p_T -uncorrelated errors, boxes around the points indicate p_T -correlated errors. Single box around $R_{AA} = 1$ on the left is the error due to N_{coll} , whereas the single box on the right is the overall normalization error of the $p + p$ reference spectrum.

$$R_{AA} = \frac{1/N_{evt} d^2N/dydp_T}{\langle T_{AB} \rangle d^2\sigma_{pp}/dydp_T} \quad (1)$$

is used, where σ_{pp} is the production cross section of the particle in $p + p$ collisions, and $\langle T_{AB} \rangle$ is the nuclear thickness function averaged over a range of impact parameters for the given centrality, calculated within a Glauber model [13]. Figures 2 and 3 show R_{AA} for π^0 at different centralities. The reference $p + p$ yield was obtained from the 2005 (Run-5) RHIC $p + p$ measurement [17].

R_{AA} reaches ~ 0.2 in 0–10% centrality at $p_T > 5$ GeV/c with very little (if any) p_T dependence. This trend is compatible with most current energy loss models but not with a semiopaque medium assumption, where R_{AA} would decrease with increasing p_T [7]. While its magnitude changes, the suppression pattern itself is remarkably similar at all centralities suggesting that the bulk R_{AA} (integrated over azimuth) is sensitive only to the N_{part} but not to the specific geometry. Consequently, study of the p_T -integrated R_{AA} vs centrality is instructive.

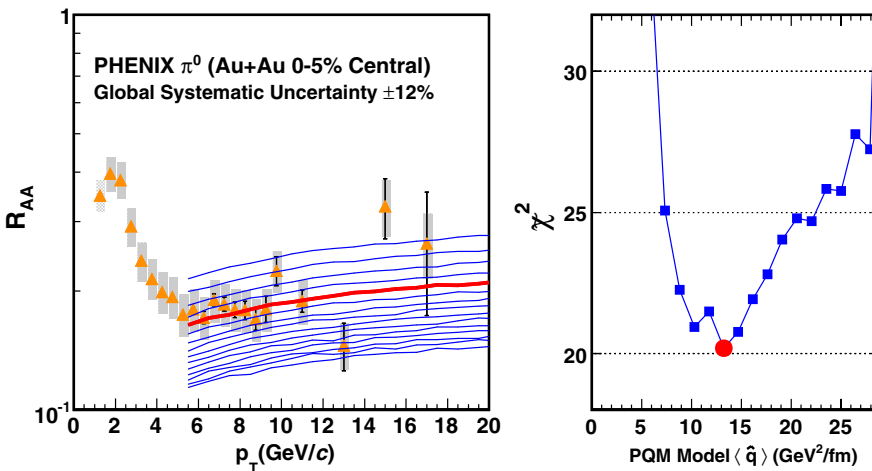


FIG. 3 (color online). Left: $\pi^0 R_{AA}$ for the most central (0–5%) Au + Au collisions and PQM model calculations for different values of $\langle \hat{q} \rangle$. Right: $\tilde{\chi}^2(\epsilon_b, \epsilon_c, p)$ distribution for the corresponding values of $\langle \hat{q} \rangle$. The bold (red) curve in the left panel and the round (red) point in the right panel are the best fit values.

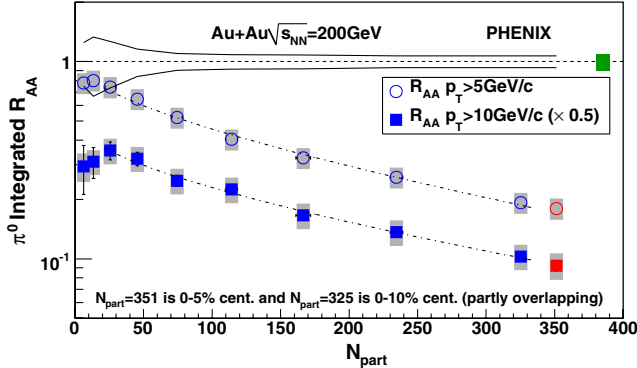


FIG. 4 (color online). Integrated nuclear modification factor (R_{AA}) for π^0 s as a function of collision centrality expressed in terms of N_{part} . The error bars/bands are the same as in Fig. 2. The two lines at unity show the errors on $\langle N_{coll} \rangle$. The last two points correspond to partially overlapping centrality bins. The dashed lines show the fit explained in the text.

Figure 4 shows R_{AA} for π^0 s integrated above $p_T > 5$ GeV/ c , and $p_T > 10$ GeV/ c , as a function of centrality. The last two points indicate overlapping 0–10% and 0–5% bins. In both cases, the suppression increases monotonically with N_{part} without any sign of saturation, suggesting that larger colliding systems (such as $U + U$ planned at RHIC) should exhibit even more suppression.

The common power-law behavior ($\propto p_T^{-n}$) in $p + p$ and Au + Au allows the suppression to be reinterpreted as a fractional energy loss $S_{loss} = 1 - R_{AA}^{1/(n-2)}$ where n is the power-law exponent, and we found that $S_{loss} \propto N_{part}^a$ [15,18]. Fitting the integrated R_{AA} with a function $R_{AA} = (1 - S_0 N_{part}^a)^{n-2}$, where n is fixed as 8.1, gives $a = 0.57 \pm 0.13$ for $N_{part} > 20$ for $p_T > 5$ GeV/ c , and $a = 0.55 \pm 0.14$ for $p_T > 10$ GeV/ c . The fit does not take errors on $p + p$ luminosity into account. The Gyulassy-Levai-Vitev (GLV) [6] and PQM [10] models predict that $a \approx 2/3$, which is consistent with the data. The fitted values of S_0 are $(9.0 \pm 6.1) \times 10^{-3}$ and $(9.4 \pm 7.3) \times 10^{-3}$ for $p_T > 5$ GeV/ c and $p_T > 10$ GeV/ c , respectively. The fits are shown as dashed lines in Fig. 4.

We use the highest centrality (0–5%) R_{AA} data as shown in Fig. 3 to constrain the PQM model parameter $\langle \hat{q} \rangle$. This must be done with careful consideration of the various, partially coupled error sources, leading to necessary refinement beyond a naive least square analysis. We calculate

$$\tilde{\chi}^2(\epsilon_b, \epsilon_c, p) = \left(\sum_{i=1}^n \frac{[y_i + \epsilon_b \sigma_{b_i} + \epsilon_c y_i \sigma_c - \mu_i(p)]^2}{\sigma_i^2} \right) + \epsilon_b^2 + \epsilon_c^2, \quad (2)$$

using theory curves $\mu_i(p)$ with different values of the input parameter p , i.e., $\langle \hat{q} \rangle$ in the PQM model. p_T -uncorrelated, statistical \oplus systematic errors are σ_i , p_T -correlated errors are σ_{b_i} (boxes on Figs. 2 and 3), while uniform fractional

shifts of all points are given by σ_c . All the measured values y_i are allowed to shift by the same fraction, ϵ_b , of their systematic error σ_{b_i} from the nominal values. The ϵ_c is a similar correlated fraction of σ_c , and $\tilde{\sigma}_i = \sigma_i(y_i + \epsilon_b \sigma_{b_i} + \epsilon_c y_i \sigma_c)/y_i$ is the point-to-point random error scaled by the multiplicative shift, so that the fractional error is unchanged by the shift, which is true for the present measurement. The best fit, $\tilde{\chi}^2_{min}$, the minimum of $\tilde{\chi}^2(\epsilon_b, \epsilon_c, p)$ by variation of ϵ_b , ϵ_c , and p , is found by standard methods. Further details are given in [16]. The right panel of Fig. 3 shows the minima of $\tilde{\chi}^2(\epsilon_b, \epsilon_c, p)$ by varying ϵ_b and ϵ_c for a wide range of values of the PQM model transport coefficient, $\langle \hat{q} \rangle$. Our data constrain $\langle \hat{q} \rangle$ as $13.2^{+2.1}_{-3.2}$ and $^{+6.3}_{-5.2}$ GeV $^2/fm$ at the 1 and 2 standard deviation levels. These constraints include only the experimental uncertainties and do not account for the large model-dependent differences in the quenching scenario and description of the medium. Extracting fundamental model-independent properties of the medium from the present data requires resolution of ambiguities and open questions in the models themselves, which also will have to account simultaneously for the p_T and centrality (average path-length) dependence. This work demonstrates the power of data for pion production in constraining the energy loss of partons. The large $\langle \hat{q} \rangle$ suggests that the matter consists of strongly coupled partons.

The $R_{AA}(p_T)$ for 0–5% was fitted with a simple linear function in the entire $p_T > 5$ GeV/ c range as well: the slope of the fit is $0.0017^{+0.0035}_{-0.0039}$ and $^{+0.0070}_{-0.0076}$ c/GeV at the 1 and 2 standard deviation levels [16]. The fact that R_{AA} as well as the power (n) for all spectra from $p + p$ to Au + Au are essentially constant proves that the dominant term in energy loss is proportional to p_T .

In summary, PHENIX has measured neutral pions in Au + Au collisions at $\sqrt{s_{NN}} = 200$ GeV at mid rapidity in the transverse momentum range of $1 < p_T < 20$ GeV/ c , analyzing high statistics data taken in 2004. The shape of the spectra is similar for all centralities, as is the shape of $R_{AA}(p_T)$ at $p_T > 5$ GeV/ c . In central collisions, the yield is suppressed by a factor of ~ 5 at 5 GeV/ c compared to the binary scaled $p + p$ reference, and the suppression prevails with little or no change up to 20 GeV/ c . The integrated R_{AA} vs centrality does not saturate at this nuclear size; also, the predicted $S_{loss} \propto N_{part}^{2/3}$ [6,10] is consistent with our data. In this picture, the energy loss increases with p_T . Using the 0–5% (most central) R_{AA} , we find that the transport coefficient $\langle \hat{q} \rangle$ of the PQM model is constrained to $13.2^{+2.1}_{-3.2} (^{+6.3}_{-5.2})$ GeV $^2/fm$ at the one (two) σ level. The experimental evidence for a high transport coefficient, derived with remarkable accuracy due to high quality data and sophisticated new analysis, as presented here and in [16], reveals a totally nontrivial feature of the dense QCD medium created at RHIC. The shape of the spectra and the suppression pattern

indicate that the dominant term in energy loss is proportional to p_T .

We thank the staff of the Collider-Accelerator and Physics Departments at BNL for their vital contributions. We acknowledge support from the Office of Nuclear Physics in DOE Office of Science and NSF (USA), MEXT and JSPS (Japan), CNPq and FAPESP (Brazil), NSFC (China), MSMT (Czech Republic), IN2P3/CNRS, and CEA (France), BMBF, DAAD, and AvH (Germany), OTKA (Hungary), DAE (India), ISF (Israel), KRF and KOSEF (Korea), MES, RAS, and FAAE (Russia), VR and KAW (Sweden), U.S. CRDF for the FSU, US-Hungarian NSF-OTKA-MTA, and US-Israel BSF.

*Deceased

[†]PHENIX Spokesperson:

jacak@skipper.physics.sunysb.edu

- [1] D. de Florian and W. Vogelsang, Phys. Rev. D **71**, 114004 (2005).
- [2] M. Gyulassy and M. Plumer, Phys. Lett. B **243**, 432 (1990).
- [3] X.-N. Wang and M. Gyulassy, Phys. Rev. Lett. **68**, 1480 (1992).

- [4] K. Adcox *et al.*, Phys. Rev. Lett. **88**, 022301 (2001).
- [5] R. Baier, Y.L. Dokshitzer, A.H. Mueller, S. Peigne, and D. Schiff, Nucl. Phys. B **484**, 265 (1997).
- [6] M. Gyulassy, P. Levai, and I. Vitev, Phys. Rev. Lett. **85**, 5535 (2000).
- [7] T. Renk, Phys. Rev. C **74**, 034906 (2006).
- [8] R. Baier and D. Schiff, J. High Energy Phys. 09 (2006) 059.
- [9] A. Dainese, C. Loizides, and G. Paic, Eur. Phys. J. C **38**, 461 (2005).
- [10] C. Loizides, Eur. Phys. J. C **49**, 339 (2007).
- [11] H. Zhang, J.F. Owens, E. Wang, and X.-N. Wang, Phys. Rev. Lett. **98**, 212301 (2007).
- [12] K. Adcox *et al.*, Nucl. Instrum. Methods Phys. Res., Sect. A **499**, 469 (2003).
- [13] M.L. Miller, K. Reygers, S.J. Sanders, and P. Steinberg, Annu. Rev. Nucl. Part. Sci. **57**, 205 (2007).
- [14] L. Aphecetche *et al.*, Nucl. Instrum. Methods Phys. Res., Sect. A **499**, 521 (2003).
- [15] S.S. Adler *et al.*, Phys. Rev. C **76**, 034904 (2007).
- [16] A. Adare *et al.*, Phys. Rev. C **77**, 064907 (2008).
- [17] A. Adare, Phys. Rev. D **76**, 051106 (2007).
- [18] K. Adcox *et al.* (PHENIX), Nucl. Phys. A **757**, 184 (2005).